Recent results on Integrable electronic models

Alberto Anfossi[1], Fabrizio Dolcini[2] and Arianna Montorsi [1]
[1] Dipartimento di Fisica and Unità INFM, Politecnico di Torino, I-10129 Torino, Italy
[2] Physikalisches Institut, Albert-Ludwigs-Universität, 79104 Freiburg, Germany
(2 December 2003)

We review the approach of generalized permutator to produce a class of integrable quantum Hamiltonians, as well as the technique of Sutherland species (SS) to map a subclass of it into solvable spinless fermions models. In particular, we apply the above scheme to construct integrable interacting electron Hamiltonians: first we review the extended Hubbard case, discussing both ground state and thermodynamics; then we pass to constrained fermion models, generating 56 integrable cases, among which both supersymmetric $t-J$ model and infinite U Hubbard model are obtained, as well as other physically interesting cases, such as a particular $t-V$ model. For the latter we describe how the complete spectrum can be gained by means of SS technique. Finally we speculate about possible applications to spin S models.

2003 PACS number(s): 71.10.Pm; 71.27.+a; 05.30.-d;02.30.Ik

I. INTRODUCTION

In recent years the discovery of materials that exhibit, at least in some energy regimes, a strong one-dimensional character has renewed the interest in models of interacting electrons in low dimensional lattices.
Conducting polymers such as polyacetylene $(CH)_x$ was probably the first noticeable example of such type of materials [1], where the interplay between π-electron correlation and chain dimerization was intensively studied [2].
Successively, a very rich temperature-pressure phase diagram has been observed for Bechgaard salts [3], which are linear-chain organic compounds such as $(TMTSF)_2X$ and $(TMTTF)_2X$, where ClO_4 or X = Br. In considerable part of their phase diagram, namely at sufficiently high temperatures and pressure, the inter-chain hopping is irrelevant and such materials actually behave as 1D systems.
More recently, huge interest has been devoted to carbon nanotubes [4], which can be regarded to as graphite cylinders of a typical radius of some nm. Due to the discrete nature of the radial motion, only one band is actually involved in determining the electronic properties (at least up to 1eV energy scales); for this reasons, as well as for the fact that they are ballistic, such materials are nowadays considered as the most promising material to probe electronic correlations in 1D.
Further significant example are semiconductor-based quantum wires synthesized through cleaved edge overgrowth [5], as well as Edge states in Fractional Quantum Hall Effect systems.

In modelling any of the above materials, it is crucial to take into account the electron-electron interaction, since the latter heavily determines their physical behavior. It is indeed well known that in low dimension *correlation* effects become important, even for moderate interaction strength; this boils down to the general fact that in 1D a single particle picture is not valid. The conventional techniques that are used in 3D to treat many body systems are therefore either unreliable (such as mean field) or inapplicable (such as Fermi Liquid theory), when investigating 1D materials. For this reason, alternative approaches have been formulated and developed, both analytical (e.g. Luttinger Liquid Theory [6]) and numerical(e.g.DMRG [7]).

In this general context, the availability of exact results for 1D electronic models (at least for some values of the model parameters) plays a crucial role, not only as a conceptual outcome, but also as a comparison test for the above 'non-traditional' techniques.

Within the exact-result approaches to one dimensional systems, the *Coordinate Bethe Ansatz* (CBA) is probably the most famous technique; it amounts to prove, when possible, that a given model Hamiltonian has eigenfunctions of the form proposed by Bethe [8]; this method has been quite successfully applied to models of correlated electrons. For instance CBA has been used for solving the Hubbard model [9] and the t-J model [10], which are somehow the prototype models to account for correlation effects in electron systems. The former reads

$$\mathcal{H}_{\rm Hub} = -t\sum_{j=1}^{L}\sum_{\sigma=\uparrow,\downarrow}(c^\dagger_{j,\sigma}c_{j+1,\sigma}+c^\dagger_{j+1,\sigma}c_{j+1,\sigma})+ \qquad (1)$$
$$+U\sum_{j=1}^{L}\hat{n}_{j,\uparrow}\hat{n}_{j,\downarrow}$$

where $c^\dagger_{j,\sigma}$ and $c_{j,\sigma}$ are electron creation and annihilation operators on a 1D lattice, j and σ label position and spin of the electons on the chain, and $\hat{n}_{j,\sigma}=c^\dagger_{j,\sigma}c_{j,\sigma}$ is the number operator. In Eqs.(1) the first term is the tight-binding part and the second the on-site Coulomb re-

pulsion competing with it. The exact solution states that any small $U > 0$ causes the ground state of the system to be insulating at half-filling, confirming the dramatic effect that correlations have in 1D.
The t-J model involves a spin-spin coupling term and its Hamiltonian reads

$$\mathcal{H}_{\rm t-J} = -t\sum_{j=1}^{L}(1-\hat{n}_{j,\bar{\sigma}})(c^{\dagger}_{j,\sigma}c_{j+1,\sigma}+h.c.)(1-\hat{n}_{j+1,\bar{\sigma}})+ \\ +J\sum_{j=1}^{L}(\vec{\mathcal{S}}_j\cdot\vec{\mathcal{S}}_{j+1}-\frac{1}{4}\hat{n}_j\hat{n}_{j+1}) \qquad (2)$$

where $\vec{\mathcal{S}} = c^{\dagger}_{j,\sigma}\frac{\vec{\sigma}_{\sigma\sigma'}}{2}c_{j,\sigma'}$ is the spin operator, and $\bar{\sigma} =\downarrow$ (resp.$\uparrow$) if $\sigma =\uparrow$ (resp.$\downarrow$). The exact solution of the t-J model for $J = 2t$ was the first analytical proof that the Luttinger liquid hypothesis for 1-D systems was well grounded. Indeed the ground state of this model, for any filling value, is a liquid of singlet bound pairs of varying spatial separation and binding energy. The excitations were actually found to be of two types: spin-like and charge-like, and they can be proved to be gapless.
The t-J model is also an example of constrained fermions, in the sense that the double occupied states are a priori excluded from the Hilbert space; this type of constraint physically emerges e.g. when investigating the low-energy singlet excitations of multi-band models; in the regime of strong correlation an effective 1-band Hamiltonian can be obtained [11,12].
A quite detailed review of CBA-solved models can be found in [13].

Beyond the CBA, there exist another quite useful technique within the framework of exact-result approaches. It is called *Quantum Inverse Scattering Method* (QISM) [14], and is in a sense more general than the CBA, in that it directly involves the notion of *integrability* of the Hamiltonian $\mathcal{H}$. Here integrability actually consists in the possibility of finding a complete set of mutually commuting observables

$$[\mathcal{J}_n\,,\,\mathcal{J}_{n'}] \,=\, 0\,, \qquad (3)$$

so that the eigenstates of $\mathcal{H}$ can be univoquely characterized by the quantum numbers related to such observables. In the QISM, all the conserved quantities are encoded in an equation, known as the Yang-Baxter-Equation (YBE); each solution of the YBE determines a specific model, endowed with a set of conserved quantities. The standard way to determine the eigenstates within the QISM is again based on an Ansatz, called Algebraic Bethe Ansatz (ABA); differently from the CBA, the ABA explicitly lies on the underlying symmetries of the Hamiltonian contained in the related YBE.

Within the above scenario, in this paper we first briefly summarize in sec.II the main ideas of the QISM applied to fermionic models; then, in sec.III we review a recently developed method [15] to determine integrable electron models. This method, formulated within the QISM, amounts to finding solutions of YBE of *polynomial* form. We show in sec.IV that already the easiest case of first order polynomial yields a rich variety of integrable models [16]. In section V we describe a technique (different from the usual ABA) to obtain the complete spectrum of the Hamiltonian for a subclass of the integrable cases. In particular, in sec.VI we review the integrable cases for extended Hubbard models (dimension of the local vector space $d_V = 4$), whereas in sec.VII we explicitly derive the integrable cases for $d_V = 3$, and look at their implementation by means of constrained fermions. Finally, in sec. VIII we give some conclusions.

II. INTEGRABILITY FOR ELECTRONIC MODELS

A. Some introductory material

In the second quantization formulation, a system of fermions on a 1D lattice is described by creation and annihilation operators, which are governed by the algebra:

$$\{c_{i,s},c_{j,s'}\}=0 \qquad \{c_{i,s},c^{\dagger}_{j,s'}\}=\delta_{i,j}\,\delta_{s,s'} \qquad (4)$$

where $s = (a, \sigma)$ is in general a multi-label, accounting for the orbital (=a) and for the spin (=σ). Here a can vary from 1 to $N_{\rm orb}$ and σ can take $2J+1$ values, where $N_{\rm orb}$ is the number of orbitals and J the (half-integer) spin.

In lattice model, one can associate to each site a local vector space V_j. As an example, in the case of s-orbital electrons we have $a = s$ and $\sigma =\uparrow,\downarrow$, V_j is made up of the 4 vectors

$$V_j = Span\Big(\,|\uparrow\rangle_j = c^{\dagger}_{j\uparrow}|o\rangle_j\,|\downarrow\rangle_j = c^{\dagger}_{j}|o\rangle_j\,; \\ |o\rangle_j\,;\,|\downarrow\uparrow\rangle_j = c^{\dagger}_{j\downarrow}c^{\dagger}_{j\uparrow}|o\rangle_j\Big) \qquad (5)$$

where $|o\rangle_j$ is the local vacuum.
More generally, V_j has dimension d_V and is spanned by vectors $|\alpha\rangle_j$

$$V_j = Span\Big(\,|\alpha\rangle_j = h^{(\alpha)}_j|o\rangle_j\,,\alpha=1\dots d_V\Big) \qquad (6)$$

Here the $h^{(\alpha)}_j$'s are products of creation operators $c^{\dagger}_{js}$ with different s [17].

An important property of fermionic systems is that, due to the anti-commutation relations (4), the space V_j has an intrinsic *graduation*; this means that V_j can be decomposed into an odd and an even subspaces

($V_j = V_j^{(1)} \oplus V_j^{(0)}$), where the odd (even) subspace $V_j^{(1)}$ ($V_j^{(0)}$) is spanned by those vectors that are built with an odd (even) number of creation operators $c_{is}^\dagger$. For instance, in the case of the s-orbital electrons, the subspace spanned by $|\uparrow\rangle_j$ and $|\downarrow\rangle_j$ is odd, and the subspace spanned by $|o\rangle_j$ and $|\downarrow\uparrow\rangle_j$ is even. Similarly, the space of local linear operators acting on V_j (denoted by $\mathrm{End}(V_j)$) is also graded; odd and even vectors and operators are also said to be parity- homogeneous; in particular they are respectively said to have parity $p = 1$ and $p = 0$, so that for any homogeneous $\mathcal{O}_j^{(a)}, \mathcal{O}_j^{(b)} \in \mathrm{End}(V_j)$ the relation $p(\mathcal{O}_j^{(a)}\,\mathcal{O}_j^{(b)}) = p(\mathcal{O}_j^{(a)}) + p(\mathcal{O}_j^{(b)})$ holds. Technically this is expressed by saying that $\mathrm{End}(V)$ is a graded local algebra.

Another important ingredient related to the vector space V_j, which plays an important role in the QISM to be presented below, is the state projectors. They are defined as

$$\mathcal{E}_{j\,\alpha}^{\ \beta} = |\alpha\rangle_{j\ j}\langle\beta| \tag{7}$$

The projectors fulfill very important properties:

$$\left[\mathcal{E}_{j\,\alpha}^{\ \beta}\,,\,\mathcal{E}_{k\,\gamma}^{\ \delta}\right]_{\pm} = 0 \qquad \forall j \neq k \tag{8}$$

$$\mathcal{E}_{j\,\alpha}^{\ \beta}\,\mathcal{E}_{j\,\gamma}^{\ \delta} = \delta_\gamma^\beta\,\mathcal{E}_{j\,\alpha}^{\ \delta} \tag{9}$$

where $[X,Y]_\pm = X\,Y - (-1)^{p(X)p(Y)}\,Y\,X$.
In the case of s-orbitals they are explicitly given by the entries ($a-$th row and the $b-$th column) of the following 4×4 matrix

$$\mathcal{E}_j = \begin{pmatrix} n_{j\uparrow}(1-n_{j\downarrow}) & c_{j\uparrow}^\dagger c_{j\downarrow} & c_{j\uparrow}^\dagger(1-n_{j\downarrow}) & c_{j\downarrow}n_{j\uparrow} \\ c_{j\downarrow}^\dagger c_{j\uparrow} & n_{j\downarrow}(1-n_{j\uparrow}) & c_{j\downarrow}^\dagger(1-n_{j\uparrow}) & -c_{j\uparrow}^\dagger n_{j\downarrow} \\ c_{j\uparrow}(1-n_{j\downarrow}) & c_{j\downarrow}(1-n_{j\uparrow}) & (1-n_{j\uparrow})(1-n_{j\downarrow}) & c_{j\uparrow}c_{j\downarrow} \\ c_{j\downarrow}^\dagger n_{j\uparrow} & -c_{j\uparrow}n_{j\downarrow} & c_{j\downarrow}^\dagger c_{j\uparrow}^\dagger & n_{j\downarrow}n_{j\uparrow} \end{pmatrix} \tag{10}$$

For constrained fermions the projector matrix is just the left upper 3×3 sub-matrix of (10).
Notice that each of the entries of the above matrix is an homogeneous operator with parity $p(\mathcal{E}_{j\,\alpha}^{\ \beta}) = p(\alpha)+p(\beta)$ [18]. Projectors are useful in decomposing any operator into its fundamental state-processes: any single-site operator $\mathcal{O}_j^{(a)}$ can indeed be written as

$$\mathcal{O}_j^{(a)} = (O^{(a)})_\beta^\alpha\,\mathcal{E}_{j\,\alpha}^{\ \beta} \tag{11}$$

where $(O^{(a)})$ is its representing matrix, defined through

$$\mathcal{O}_j^{(a)}\,|\beta\rangle_j = (O^{(a)})_\beta^\alpha\,|\alpha\rangle_j \tag{12}$$

B. Quantum Inverse Scattering Method for fermions: a short and schematic review

The Quantum Inverse Scattering Method (QISM) is a powerful tool for studying quantum integrability because it provides models endowed with a set of mutually commuting operators. Within the QISM a key role is played by the Yang-Baxter Equation (YBE)

$$\begin{aligned}&(\mathbf{I}\otimes\check{R}(u-v))\,(\check{R}(u)\otimes\mathbf{I})\,(\mathbf{I}\otimes\check{R}(v)) = \\ &= (\check{R}(v)\otimes\mathbf{I})\,(\mathbf{I}\otimes\check{R}(u))\,(\check{R}(u-v)\otimes\mathbf{I})\end{aligned} \tag{13}$$

Here $\check{R}$ is a $d_V^2\times d_V^2$ C-number matrix, and $\mathbf{I}$ is the $d_V\times d_V$ identity matrix (d_V being the dimension of the local vector space V_j); $\check{R}$ depends on the complex number u (called spectral parameter), and thus the YBE is a functional equation for $\check{R}$.

To each solution of the YBE one can associate an integrable model; here below we shall briefly describe how to obtain integrable *fermionic* models (fermionic QISM, for more details see Ref. [19,20]).
From the $\check{R}$-matrix one can construct an operator-valued matrix $\mathcal{L}_j$, related to each site j, as follows

$$\mathcal{L}_{|\,\beta}^{\ \alpha}(u) = (-1)^{p(\alpha)p(\gamma)}\,\check{R}_{\beta\delta}^{\gamma\alpha}(u)\,\mathcal{E}_{j\,\gamma}^{\ \delta} \tag{14}$$

where the $\mathcal{E}_{j\,\gamma}^{\ \delta}$ are the projectors (7). Here α gives the row and β the column of the entry of the $\mathcal{L}_j$ matrix (usually called $\mathcal{L}$-operator). Due to eqn.(8) the entries of two operators $\mathcal{L}_j$ and $\mathcal{L}_k$ of different sites fulfill

$$\left[\mathcal{L}_{j\,\beta}^{\ \alpha}(u), \mathcal{L}_{k\,\delta}^{\ \gamma}(u')\right]_{\pm} = 0 \quad \forall\alpha,\beta,\gamma,\delta \quad \forall u,u' \quad \forall j\neq k \tag{15}$$

At the same time the property (9) of the projectors allows to show that the Yang-Baxter equation (13) is actually equivalent to

$$\begin{aligned}\check{R}(u-v)\,(\mathcal{L}_j(u)\otimes_s\mathcal{L}_j(v)) = \\ = (\mathcal{L}_j(v)\otimes_s\mathcal{L}_j(u))\,\check{R}(u-v)\end{aligned} \tag{16}$$

where the symbol $\otimes_s$ is called *graded* tensor product, and it is defined as

$$(\mathcal{A}\otimes_s\mathcal{B})_{(\{\beta\},\{\delta\})}^{(\{\alpha\},\{\gamma\})} = \mathcal{A}_{\{\beta\}}^{\{\alpha\}}\,\mathcal{B}_{\{\delta\}}^{\{\gamma\}}\,(-1)^{(p(\{\alpha\})+p(\{\beta\}))\,p(\{\gamma\})} \tag{17}$$

The presence of the above additional signs is strictly related to the fermionic nature of the system, as observed in II A.
Eq.(16) is a local relation, in that it only involves the j-th site of the 1D lattice. However, using the property

$$(\mathcal{L}_i \otimes_s \mathcal{L}_j)(\mathcal{L}_k \otimes_s \mathcal{L}_l) = (\mathcal{L}_i \mathcal{L}_k \otimes_s \mathcal{L}_j \mathcal{L}_l) \qquad \forall\, j \neq k \quad (18)$$

one can easily show that

$$\begin{aligned} \check{R}(u-v)\,(\mathcal{T}(u) \otimes_s \mathcal{T}(v)) \;= \\ = (\mathcal{T}(v) \otimes_s \mathcal{T}(u))\,\check{R}(u-v), \end{aligned} \quad (19)$$

where

$$\mathcal{T}(u) = \mathcal{L}_L(u) \ldots \mathcal{L}_2(u) \mathcal{L}_1(u) \quad (20)$$

Notice that $\mathcal{T}(u)$ is a operator-valued matrix (usually called monodromy matrix), whose entries are now operators defined on the whole 1D chain.
Eq.(19) is the main relation of the QISM, because taking the trace of $\mathcal{T}(u)$ yields

$$[tr\,\mathcal{T}(u), tr\,\mathcal{T}_N(v)] = 0 \qquad \forall u, v \quad (21)$$

which already implies the existence of an infinite number of conservation laws; indeed developing the operator $tr\,\mathcal{T}(u)$ in powers of u, eq.(21) states that all the coefficients (i.e. operators defined on the chain) mutually commute.
Typically one searches for solutions of the YBE with the 'boundary condition' that for a given point u_0, $\check{R}(u)$ is the identity matrix

$$\check{R}^{\alpha\gamma}_{\beta\delta}(u_0) = \delta^\alpha_\beta\, \delta^\gamma_\delta \quad (22)$$

In this case one typically introduces

$$\mathcal{Z}(u) := (tr\,\mathcal{T}(u_0))^{-1}\, tr\,\mathcal{T}(u) \quad (23)$$

and defines

$$\mathcal{J}_n \;=\; \frac{d^n}{du^n} \ln \mathcal{Z}(u)\Big|_{u=u_0} \qquad n \geq 1 \quad . \quad (24)$$

Eq.(21) therefore implies

$$[\,\mathcal{J}_n\,,\,\mathcal{J}_{n'}\,] = 0 \quad (25)$$

where $\mathcal{J}_n$ are the mutually conserved quantities. It can be shown that $\mathcal{J}_n$ is the sum of operators involving clusters of no more than $n+1$ sites [21].
The first conserved quantity $\mathcal{J}_1$ is usually interpreted as the Hamiltonian, and the other ones as its symmetries. $\mathcal{J}_1$ has the form

$$\mathcal{J}_1 = \mathcal{H} = \sum_{j=1}^{L} \mathcal{H}_{j\,j+1} \quad (26)$$

with periodic boundary conditions $\mathcal{H}_{L\,L+1} = \mathcal{H}_{L\,1}$.
Each $\mathcal{H}_{j\,j+1}$ is a two-site Hamiltonian, and it is straightforwardly connected with the $\check{R}$-matrix solution of the YBE. Explicitly one can show that

$$\begin{aligned} &\mathcal{H}_{j\,j+1} = \\ &= (-1)^{p(\gamma)(p(\beta)+p(\delta))}\, \partial_u \check{R}^{\alpha\beta}_{\gamma\delta}(u)\Big|_{u=u_0}\, \mathcal{E}_{j\,\alpha}^{\;\gamma}\, \mathcal{E}_{j+1\,\beta}^{\;\;\delta} \end{aligned} \quad (27)$$

Writing down the 2-site Hamiltonian $\sum_j \mathcal{H}_{j\,j+1}$ in a matrix representation $H_{j\,j+1}$, the relation with the $\check{R}$-matrix looks even simpler, namely

$$(H_{2\,\text{sites}})^{\alpha\beta}_{\gamma\delta} = \partial_u \check{R}^{\alpha\beta}_{\gamma\delta}(u)\Big|_{u=u_0} \quad (28)$$

III. POLYNOMIAL R-MATRIX TECHNIQUE

In the previous section we showed that to each solution $\check{R}$ of the YBE (13) one can associate a fermionic Hamiltonian $\mathcal{H} = \mathcal{H}_{j\,j+1}$ endowed with a set of symmetries $\mathcal{J}_n$'s. The derivative of $\check{R}$ with respect to u basically represents the two-site Hamiltonian $\mathcal{H}_{j\,j+1}$ through the relations (40) (operatorial form) or (28) (matrix representation).
The purpose is now to find solutions of the YBE, to figure out what kind of Hamiltonian is associated to the solution and to determine its physical features. Here below we describe a technique that we recently developed to find solutions of the YBE, and then we describe what kind of models we obtain.
Notice that if $\check{R}(u)$ is a solution of (13) then $\check{R}' = f(u)\check{R}(u)$, with $f(u)$ any scalar function satisfying $f(0) = 1$, is a solution as well, and it corresponds to an Hamiltonian $\mathcal{H}' = \mathcal{H} + \rfloor\, \mathbf{I}$ where $c = \frac{df}{du}|_{u=0}$.

Our approach consists in looking for solutions of (13) which are polynomials in the spectral parameter and satisfy (22) for $u_0 = 0$. This implies:

$$\check{R}(u) = \mathbf{I} + u(H_{2\,\text{sites}} + c\,\mathbf{I}) + \frac{u^2}{2!}\check{R}^{(2)} + \ldots + \frac{u^p}{p!}\check{R}^{(p)} \quad , \quad (29)$$

with p the degree of the polynomial (unknown *a priori* and possibly infinite). Here $\check{R}^{(i)}\,(i = 1, \ldots, p)$ are unknown coefficients which are to be fixed through eqn.(13) and $\mathbf{I}$ the $d_V^2 \times d_V^2$ identity matrix.

Let us substitute the Ansatz (29) into eqn (13); due to the fact that YBE must be satisfied $\forall u, v$, we have to equate all the coefficients of the same power $u^n\, v^m$. Thus we end up with *algebraic* equations, which can be grouped order by order, the order being the value $l = m + n$. The *Zero*-th and *First Order* equations are mere identities which are always satisfied. For the *Second Order* we have

$$\check{R}^{(2)} = (\check{R}^{(1)})^2 + \mathbf{I}\delta \quad (30)$$

where $\check{R}^{(1)} = H + c\mathbf{I}$, and δ, c are constants to be determined.

The *Third Order* case still reduces to a single equation, which reads

$$\left\{\check{R}^{(1)}_{12}, \check{R}^{(2)}_{23}\right\} - \check{R}^{(1)}_{23}\check{R}^{(2)}_{23} - 2\check{R}^{(1)}_{23}\,\check{R}^{(1)}_{12}\,\check{R}^{(1)}_{23} + \check{R}^{(3)}_{23} =$$
$$= \left\{\check{R}^{(1)}_{23}, \check{R}^{(2)}_{12}\right\} - \check{R}^{(1)}_{12}\check{R}^{(2)}_{12} - 2\check{R}^{(1)}_{12}\,\check{R}^{(1)}_{23}\,\check{R}^{(1)}_{12} + \check{R}^{(3)}_{12} \quad , \quad (31)$$

where $\{\ ,\ \}$ is the anticommutator.

The successive orders in general consist of more equations, up to the *Highest Order* $3p$, in which case the equation is simply the (spectral parameter independent) YBE,

$$\check{R}^{(p)}_{23}\,\check{R}^{(p)}_{12}\,\check{R}^{(p)}_{23} = \check{R}^{(p)}_{12}\,\check{R}^{(p)}_{23}\,\check{R}^{(p)}_{12} \quad (32)$$

Notice that, as the second order equation (30) is explicitly solved once the Hamiltonian is given, the non trivial equations start from the third order; for a polynomial of degree $p \geq 1$ one has $3p-2$ actual orders to consider.
The idea is to proceed by successive attempts: once the Hamiltonian $\mathcal{H}$ is given, one first tries to solve the equations by means of a first order polynomial $\check{R}$ -matrix; if this is not possible one passes to a second order polynomial and so on. If the Ansatz (29) is correct one can hope to find the $\check{R}$-matrix in a finite number of steps, or guessing a recursive formula for the coefficient $\check{R}^{(i)}$. The advantage of this method is that it deals with *algebraic* equations instead of functional equations (cfr.(13)).

The simplest non-trivial case of a polynomial R-matrix is of course obtained for $p = 1$. In this case $\check{R}(u) = \mathbf{I} + u\check{R}^{(1)}$, and, due to (32), $\check{R}^{(1)}$ is nothing but a braid operator. Moreover, eq. (30) implies that the square of $\check{R}^{(1)}$ is proportional to the identity (since $\check{R}^{(2)} = 0$ for a first order polynomial)

$$(\check{R}^{(1)})^2 \propto \mathbf{I} \quad (33)$$

Eqs.(32) and (33) imply that $\check{R}^{(1)}$ (and hence the Hamiltonian $\mathcal{H}$) is in fact an element of the symmetric group. The solutions of the symmetric group relations have been fully investigated for a two-dimensional local space (see for instance [22]); whereas the case of dimension $d_V = 4$ of the local vector space V was considered in [16], [20]. In the next section we extend the latter approach to generic dimension d_V.

IV. GENERALIZED PERMUTATOR R-MATRICES

It is well known that, among the solutions of the symmetric group relations (32)-(33), one always finds the permutation operator P, defined by $P(e_\alpha \otimes e_\beta) = e_\beta \otimes e_\alpha$, where the e_α's for $\alpha = 1, \ldots, d_V$ form an orthonormal basis for the local vector space V. In fact, this is true whatever the dimension of the representation is, and also holds for any *graded* permutation operator P_g, where $P_g(e_\alpha \otimes e_\beta) = (-)^{\epsilon(\alpha)\epsilon(\beta)} e_\beta \otimes e_\alpha$, with $\epsilon_\alpha = 0, 1$ grading of the vector e_α. Therefore, both P and P_g give rise to integrable models. One may wonder whether there are other solutions of symmetric group relations generalizing the structure of P, P_g. Here we propose the *generalized permutator* ones, given by operators Π which either transform one product of basis vectors into the reversed product, or leave it unchanged, according to a rule explained below. In the matrix form this means that there is precisely one non-zero entry in each column and row of Π. Moreover, due to (33), the non-vanishing entries of Π must be equal to $+1$ or -1, up to an overall multiplicative constant. Explicitly, $\forall \alpha, \beta = 1, \ldots d_V$,

$$\Pi(e_\alpha \otimes e_\beta) = \underbrace{\theta^d_{\alpha\beta}(e_\alpha \otimes e_\beta)}_{\text{diagonal terms}} + \underbrace{\theta^o_{\alpha\beta}\,(e_\beta \otimes e_\alpha)}_{\text{off-diagonal terms}} \quad . \quad (34)$$

Here $\theta^d_{\alpha\beta} = \epsilon_{\alpha\beta} s^d_{\alpha\beta}$, and $\theta^o_{\alpha\beta} = (1 - \epsilon_{\alpha\beta}) s^o_{\alpha\beta}$, where $\epsilon_{\alpha\beta}$ is a discrete (0 or 1) valued function satisfying $\epsilon_{\alpha\beta} = \epsilon_{\beta\alpha}$ and $\epsilon_{\alpha\alpha} = 1$, which selects the diagonal/off-diagonal terms; moreover, $s^d_{\alpha\beta} = \pm 1$ accounts for additional signs of the diagonal entries, while $s^o_{\alpha\beta} = \pm 1$ stands for the signs of off-diagonal terms; we shall impose $s^o_{\alpha\beta} = s^o_{\beta\alpha}$ in order to make Π a symmetric matrix.

It can be easily verified that the operators Π have square equal to the identity. Moreover, let us denote by $\mathcal{S}$ the set of index values, *i.e.* $\mathcal{S} = \{1, \ldots, d_V\}$; the function $\epsilon_{\alpha\beta}$ on $\mathcal{S} \times \mathcal{S}$ characterizes the structure of any Π. Let us denote by $\mathcal{A}^d$ the subset of $\mathcal{S} \times \mathcal{S}$ of the couples (α, β) for which $\epsilon_{\alpha\beta} = 1$: they determine the positions $4(\alpha - 1) + \beta$ of the non-vanishing *diagonal* entries; since $\epsilon_{\alpha\beta} = \epsilon_{\beta\alpha}$, whenever $\theta^d_{\alpha\beta} \neq 0$ we also have that $\theta^d_{\beta\alpha} \neq 0$; in other words, the subset $\mathcal{A}^d$ can always be written in the form $\mathcal{A}^d = \bigcup_i \mathcal{S}_i \times \mathcal{S}_i$ where the $\mathcal{S}_i$'s are disjoint subsets of $\mathcal{S}$, with $i = 1, \ldots, N_S$, and $N_S \leq d_V$ number of disjoint subsets in S .
Inserting Π into the relation (32) it can be easily found that it is a solution if and only if $\theta^d_{\alpha\beta} = p_i \quad \forall\, (\alpha, \beta) \in \mathcal{S}_i \times \mathcal{S}_i$, where $p_i = \pm 1$ are signs. The values of the p_i's can be chosen independently, and the remaining off-diagonal non-vanishing entries are also free. In the following we shall refer to these solutions as the generalized permutators, and with abuse of notation we still denote them as Π.
Notice that this class of solutions exists for arbitrary d_V, and in fact their actual number is an increasing function of d_V. As an example, in the next sections we shall investigate how these solutions provide 1440 integrable models in case of fermionic realizations with $d_V = 4$ (unconstrained fermions with two flavors), and 56 models in case of two flavors constrained fermions ($d_V = 3$). At this stage, however, each of the integrable models proposed has no free parameter; we shall discuss in the next paragraphs how this limit can be partly removed by adding to the generalized permutators conserved quantities with

free parameters. Of course, the actual number of the latter will depend again on the dimension of the local vector space.

V. SUTHERLAND SPECIES AND SPECTRUM

The meaning of a generalized permutator is easily understood in terms of so called Sutherland species (SS). Starting from a given local vector space V, we may think to group its d_V basis vector e_α (which in the sequel we shall denote as physical species PS) into $N_S \leq d_V$ different species $\mathcal{S}_i$ which we call Sutherland species. Each of these species is left unchanged by the action of the generalized permutator, the latter interchanging only basis vector belonging to different SS's. A generalized permutator would then have the structure of an ordinary permutator if represented on a local vector space of dimension N_S. Notice that, with respect to this interpretative scheme, apparently the solutions presented in the previous section allow some extra freedom in the choice of signs of non-diagonal elements; on the contrary, here the off-diagonal elements connecting different PSs of the same SS S_i to a different SS S_j must have the same sign, say s_i. Such difference disappears through a redefinition of phase of some basis vectors belonging to $S_i \otimes S_j$.

The only signs in (34) which cannot be changed by a mere redefinition of basis are those of diagonal elements. Indeed, these signs can be used to classify the different Π solutions of GYBE for a given dimension d_V. Following Sutherland's notation [23], each species can be classified as either 'fermionic'(F) or 'bosonic'(B), according to the sign of diagonal elements. Hence all integrable models given in (34) are of type

$$F^{N_S-l}B^l \quad , \quad l=0,\ldots,N_S \quad , \quad 2 \leq N_S \leq d_V \quad , \quad (35)$$

and characterize a model with $N_S - l$ fermionic and l bosonic SS's. Different models that are recognized to be of the same SS-types also share the same structure of Coordinate or Algebraic Bethe Ansatz equations. The number of different types of such structures associated with the generalized permutators can be easily evaluated, and is

$$\nu(d_V) = \frac{1}{2}d_V^2 + \frac{3}{2}d_V - 2 \quad , \quad (36)$$

for given d_V. We remark that this is not to be confused with the number of different integrable Hamiltonians which in general is greater.

The cases F^P and BF^P have have been investigated in [23] within the framework of the Coordinate Bethe Ansatz, and ground state energy equations have been obtained. Moreover, the cases F^P and B^P have been explicitly examined in [24] within the QISM; and some other cases (BF^2 and B^2F^2) share the same algebraic structure as known models ($t-J$ [25,26] and EKS [27] respectively).
In particular, for the BF type of models, the entire spectrum can be obtained, and coincide, up to constant terms, with that of spinless fermions on an open chain:

$$E(\{n_l\}) = -2\sum_{l=1}^{L} \cos\left(\frac{\pi l}{L+1}\right) n_l \quad , \quad (37)$$

where $n_l = 0, 1$ are quantum numbers and L the length of the chain.
Notice that in the latter case we have the spectrum for any d_V. This means that in particular the ground state energy is independent of d_V. However, it must be realized that the actual degeneracy of each eigenvalue depends on the way the Sutherland's species are realized in terms of physical species for each specific model. This enters explicitly the calculation of both the ground state energy and the partition function, determining different physical features of models with the same FB structure, as we shall discuss for the case $d_V = 4$ in a subsequent section.
Within the spectrum, the ground state is particularly worth of interest, because these Hamiltonians are expected to well describe materials that exhibit peculiar physics at low temperatures. For the F^P case, it can be shown [23] that the miminum of the energy, whose eigenvalue reads

$$\epsilon_0 = 1 - \frac{2}{P}\int_0^1 dx\, \frac{x^{\frac{1}{P}-1}-1}{1-x} \quad , \quad (38)$$

is reached at equal densities of all fermionic species.
Also, again as far as the ground state is concerned, it has been shown [28] that Sutherland's theorem (originally formulated for permutators of physical species) can be extended to the generalized permutators, and it is thus possible to assert that, in the thermodynamic limit, the ground state energy (per site) ϵ_0 of a B^nF^m problem is equal to that of a BF^m problem, for which the Bethe Ansatz equation have been formulated in full generality in [23].

VI. APPLICATIONS TO EXTENDED HUBBARD MODELS

Here we review how the generalized permutator approach succeeds in producing a class of integrable models when applied to Hubbard-like systems of interacting electrons.

A. Hamiltonian and representation

We consider here a quite general 1-band extended isotropic Hubbard model preserving the total spin and number N of electrons, which reads

$$\mathcal{H} = -\sum_{\langle j,k\rangle,\sigma}[t - X(\hat{n}_{j,-\sigma}+\hat{n}_{k,-\sigma}) + \tilde{X}\hat{n}_{j,-\sigma}\hat{n}_{k,-\sigma}]c^{\dagger}_{j,\sigma}c_{k,\sigma} + U\sum_{j}\hat{n}_{j,\uparrow}\hat{n}_{j,\downarrow} + \frac{V}{2}\sum_{\langle j,k\rangle}\hat{n}_j\hat{n}_k - \mu\sum_j\hat{n}_j \tag{39}$$
$$+\frac{W}{2}\sum_{\langle j,k\rangle,\sigma,\sigma'}c^{\dagger}_{j,\sigma}c^{\dagger}_{k,\sigma'}c_{j,\sigma'}c_{k,\sigma} + Y\sum_{\langle j,k\rangle}c^{\dagger}_{j,\uparrow}c^{\dagger}_{j,\downarrow}c_{k,\downarrow}c_{k,\uparrow} + P\sum_{\langle j,k\rangle}\hat{n}_{j,\uparrow}\hat{n}_{j,\downarrow}\hat{n}_k + \frac{Q}{2}\sum_{\langle j,k\rangle}\hat{n}_{j,\uparrow}\hat{n}_{j,\downarrow}\hat{n}_{k,\uparrow}\hat{n}_{k,\downarrow}\,,$$

In (39) t represents the hopping energy of the electrons, while the subsequent terms describe their Coulomb interaction energy in a narrow band approximation: U parametrizes the on-site repulsion, V the neighboring site charge interaction, X the bond-charge interaction, W the exchange term, and Y the pair-hopping term. Moreover, additional many-body coupling terms have been included in agreement with [29]: $\tilde{X}$ correlates hopping with on-site occupation number, and P and Q describe three- and four-electron interactions. Finally, μ is the chemical potential.

The local vector space V at each lattice site has $d_V = 4$, and in the following we shall identify the 4 physical states $|\uparrow\rangle$, $|\downarrow\rangle$, $|0\rangle$ and $|\downarrow\uparrow\rangle$ with the canonical basis e_α of C^4.

The matrix representation of the two-site Hamiltonian $\mathcal{H}_{j,j+1}$ can be obtained through the projectors (10) in the following way

$$\mathcal{H}_{j\,j+1} = (-1)^{p(\gamma)(p(\beta)+p(\delta))}(H^{(2)}_{EH})^{\alpha\beta}_{\gamma\delta}\;\mathcal{E}_{j\,\alpha}^{\ \gamma}\,\mathcal{E}_{j+1\,\beta}^{\ \ \delta} \tag{40}$$

Explicitly

$$H^{(2)}_{EH} = \left(\begin{array}{cccc|cccc|cccc|cccc}
h^{11}_{11} & 0 & 0 & 0 & 0 & 0 & 0 & 0 & 0 & 0 & 0 & 0 & 0 & 0 & 0 & 0\\
0 & h^{12}_{12} & 0 & 0 & h^{12}_{21} & 0 & 0 & 0 & 0 & 0 & 0 & h^{12}_{34} & 0 & 0 & h^{12}_{43} & 0\\
0 & 0 & h^{13}_{13} & 0 & 0 & 0 & 0 & 0 & h^{13}_{31} & 0 & 0 & 0 & 0 & 0 & 0 & 0\\
0 & 0 & 0 & h^{14}_{14} & 0 & 0 & 0 & 0 & 0 & 0 & 0 & 0 & h^{14}_{41} & 0 & 0 & 0\\
- & - & - & - & - & - & - & - & - & - & - & - & - & - & - & -\\
0 & h^{12}_{21} & 0 & 0 & h^{21}_{21} & 0 & 0 & 0 & 0 & 0 & 0 & h^{21}_{34} & 0 & 0 & h^{21}_{43} & 0\\
0 & 0 & 0 & 0 & 0 & h^{22}_{22} & 0 & 0 & 0 & 0 & 0 & 0 & 0 & 0 & 0 & 0\\
0 & 0 & 0 & 0 & 0 & 0 & h^{23}_{23} & 0 & 0 & h^{23}_{32} & 0 & 0 & 0 & 0 & 0 & 0\\
0 & 0 & 0 & 0 & 0 & 0 & 0 & h^{24}_{24} & 0 & 0 & 0 & 0 & 0 & h^{24}_{42} & 0 & 0\\
- & - & - & - & - & - & - & - & - & - & - & - & - & - & - & -\\
0 & 0 & h^{13}_{31} & 0 & 0 & 0 & 0 & 0 & h^{31}_{31} & 0 & 0 & 0 & 0 & 0 & 0 & 0\\
0 & 0 & 0 & 0 & 0 & 0 & h^{23}_{32} & 0 & 0 & h^{32}_{32} & 0 & 0 & 0 & 0 & 0 & 0\\
0 & 0 & 0 & 0 & 0 & 0 & 0 & 0 & 0 & 0 & 0 & 0 & 0 & 0 & 0 & 0\\
0 & h^{12}_{34} & 0 & 0 & h^{21}_{34} & 0 & 0 & 0 & 0 & 0 & 0 & h^{34}_{34} & 0 & 0 & h^{34}_{43} & 0\\
- & - & - & - & - & - & - & - & - & - & - & - & - & - & - & -\\
0 & 0 & 0 & h^{14}_{41} & 0 & 0 & 0 & 0 & 0 & 0 & 0 & 0 & h^{41}_{41} & 0 & 0 & 0\\
0 & 0 & 0 & 0 & 0 & 0 & 0 & h^{24}_{42} & 0 & 0 & 0 & 0 & 0 & h^{42}_{42} & 0 & 0\\
0 & h^{12}_{43} & 0 & 0 & h^{21}_{43} & 0 & 0 & 0 & 0 & 0 & 0 & h^{34}_{43} & 0 & 0 & h^{43}_{43} & 0\\
0 & 0 & 0 & 0 & 0 & 0 & 0 & 0 & 0 & 0 & 0 & 0 & 0 & 0 & 0 & h^{44}_{44}
\end{array}\right) \tag{41}$$

where

$$h^{11}_{11} = h^{22}_{22} = \mu + V - W \qquad h^{12}_{12} = h^{21}_{21} = \mu + V \qquad h^{13}_{13} = h^{31}_{31} = h^{23}_{23} = h^{32}_{32} = \mu/2$$
$$h^{12}_{21} = W \qquad h^{34}_{43} = Y \qquad h^{13}_{31} = h^{23}_{32} = -t \qquad h^{14}_{41} = h^{24}_{42} = t - 2X + \tilde{X}$$
$$h^{14}_{14} = h^{41}_{41} = h^{24}_{24} = h^{42}_{42} = \frac{3}{2}\,\mu + P + \frac{U}{2} + 2V - W \qquad h^{34}_{34} = h^{43}_{43} = \mu + \frac{U}{2} \tag{42}$$
$$h^{44}_{44} = 2\mu + 4P + Q + U + 4V - 2W \qquad h^{12}_{34} = h^{12}_{43} = -h^{21}_{34} = -h^{21}_{43} = t - X \quad .$$

B. Integrable cases

We would like to recognize in the matrix (41) one of the generalized permutators given in section 3. According to the scheme discussed there, this would guarantee that the corresponding Hamiltonian is then integrable. We first observe that this correspondence is possible only if $t - X = 0$; indeed only in this case the non vanishing entries of $H^{(2)}_{EH}$ may coincide with those of a generalized permutator. When this condition is implemented, the representation of the two-site extended Hubbard Hamiltonian (up to an additive constant c) is itself a generalized permutator whenever some linear relations among the non-vanishing Hamiltonian entries and the non-vanishing elements of a generalized permutator are satisfied. It turns out that actually there are 96 different possible choices of values of the physical parameters in $\mathcal{H}$ satisfying such relations. They can be cast into six groups as (43) shows.

	$H_1(s_1,\ldots,s_5)$	$H_2(s_1,\ldots,s_5)$	$H_3(s_1,s_2,s_3)$	$H_4(s_1,s_2,s_3)$	$H_5(s_1,s_2,s_3)$	$H_6(s_1,s_2,s_3)$
t	1	1	1	1	1	0
X	1	1	1	1	1	0
$\tilde{X}$	$1+s_2$	$1+s_2$	$1+s_2$	$1+s_2$	1	1
U	$2s_1$	$2s_1$	$4s_1$	$4s_1$	$2s_1$	$-2s_1$
V	s_1	s_1+s_4	s_1	s_1+s_3	s_1+s_3	0
W	s_4	0	s_3	0	0	0
Y	s_3	s_3	0	0	s_2	s_2
P	s_4-s_1	$-s_1-2s_4$	s_3-2s_1	$-2(s_1+s_3)$	$-(s_1+s_3)$	0
Q	$-2s_4+s_1+s_5$	$4s_4+s_1+s_5$	$4s_1-2s_3$	$4(s_1+s_3)$	s_1+s_3	s_1+s_3
μ	$-2s_1$	$-2s_1$	$-2s_1$	$-2s_1$	$-2s_1$	0

(43)

Here $s_i = \pm 1$, $i = 1,\ldots,5$ are arbitrary signs; the first two groups consist of 32 different solutions each, while any of the other four groups is made of 8 different cases. Notice that requiring the conservation of spin has reduced the 1440 generalized permutators solutions of YBE for $d_V = 4$ down to the present 96 solutions described in (43).

As expected, $t = X$ is a common feature exhibited by all the solutions, implying that the number of doubly occupied sites is a conserved quantity for those $\mathcal{H}$ that are derivable from first-degree polynomial R-matrices. This feature is important in that it means that in these cases $\mathcal{H}$ can be diagonalized within a sector with a given number of up and down electrons and doubly occupied sites. In practice, the solvability of the model in one dimension is not affected by having values of U and μ in $\mathcal{H}$ other than those reported in (43) (see also [27]), as well as by the presence of an external magnetic field (*i.e.* adding to $\mathcal{H}$ a term proportional to $\sum_j n_{j,\uparrow} - n_{j,\downarrow}$).

The 96 integrable cases given in (43) can be classified according to the scheme of SS's, which allow to distinguish just 12 different algebraic structures. In particular, the first group is characterized by $N_S \equiv d_V (= 4)$ SS's, hence all models are of type $F^{4-l}B^l$; whereas the second and the third group correspond to $N_S = 3$ SS's, and the remaining three groups all correspond to $N_S = 2$ SS's. To all these structures are associated different sets of Bethe Ansatz equations, which have been explicitly worked out in [30], even though not explicitly solved. In what follows we illustrate a different approach to some of these algebraic structures, which allow an explicit evaluation of many physical features.

C. Ground state and thermodynamics

Recognizing that a model identifies (up to some commuting terms) a set of Sutherland Species greatly simplifies the calculation of the spectrum. The crucial point which allows that is the use of *open* boundary conditions, instead of the customary periodic ones; although in the thermodynamic limit the bulk properties are not affected by either choice, the calculations are more straightforward for the former. Indeed in an open one-dimensional chain the set of eigenvalues of a generalized permutator is equal to that of an ordinary permutator between N_S objects, i.e. the effective dimensionality of the Hilbert space is reduced (reduction theorem). As a consequence of that, the degeneracy of the eigenvalues can also be computed, simply counting the ways one can realize a given configuration of Sutherland Species.

The reduction theorem is proved when realizing that, according to what observed above, the relative order of any sequence of states belonging to the same species is preserved [31]; the Hamiltonian can therefore be diagonalized within each subspace of given set of sequences. For instance, for $N_S = 2$ any model of FB type has a spectrum given by (38) (plus conserved quantities), and the ground state energy per site is simply obtained by filling all the lower energy levels up to the Fermi level; it turns out to be just a function of the total number of F particles in the ground state, n_F, and it reads

$$\epsilon_0(n_F) = 2n_F - \frac{2}{\pi} sin(\pi n_F) + (U - \bar{U}) n_{\uparrow,\downarrow} + (\mu - \bar{\mu}) n \quad ; \tag{44}$$

here $\bar{U}$, and $\bar{\mu}$ are the value of U and μ as fixed from table (43), $n = \frac{1}{L}\sum_j \hat{n}_j$, and $n_{\uparrow,\downarrow} \doteq \frac{1}{L}\sum_j \hat{n}_{j,\uparrow}\hat{n}_{j,\downarrow}$ is itself a function of n_F, the explicit form of which depends on the specific FB model we are looking at. Hence, the true ground state energy of the model is obtained by minimizing (44) with respect to n_F, and will depend on the physical parameter n and U. This is shown in fig (1)-(2).

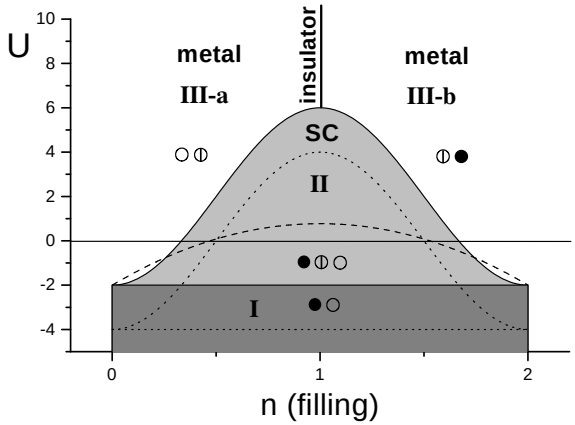

FIG. 1. Ground state phase diagram of models with a single doubly degenerate SS of type F; for all models $t = X = 1$. Moreover the continuous lines describe the case $\tilde{X} = (1 - \sigma)$; $Y = -\sigma$; $P = -1$; $Q = 2$ [28] ; the dashed line is the EKS model [27] ($\tilde{X} = W = Y = V = 1$, $P = Q = 0$), and the dotted line corresponds to the AAS model ($\tilde{X} = W = Y = V = P = Q = 0$ [31]). All models exhibit an insulator-superconductor transition at $n = 1$, for different U_c.

There we plot the ground state phase diagram for different FB models, in which $t = X = 1$, U and n are varied, and the other interaction parameters are chosen in different specified ways, so as to have, within the same F species, two PS for (1), and three PS for (2).
The empty circles represent empty states, the barred circles represent singly occupied states, the full circles are doubly occupied states; regions in which there are no singly occupied states are characterized by $n_F = 0$.

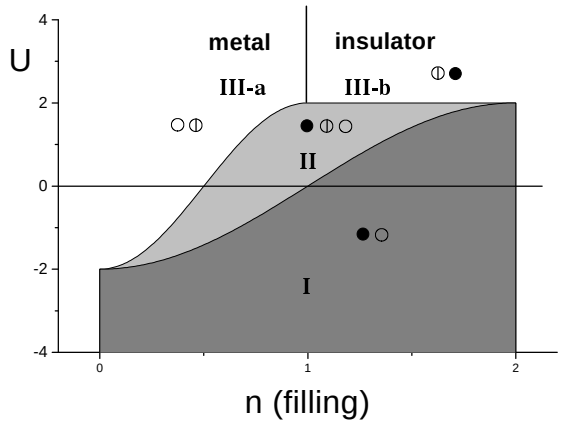

FIG. 2. Ground state phase diagram of the model $X = \tilde{X} = 1$; $Y = \sigma$; $V = W = P = Q = 0$. A filling controlled metal-insulator transition takes place for $U \geq 2$ between two *finite* regions, III-a and III-b.

The dramatic differences in the phase diagram of models represented in the figures are simply due to the fact that in the first case the F species contains two physical species ($|\uparrow\rangle$, and $|\downarrow\rangle$), implying $n_{\uparrow,\downarrow} = \frac{1}{2}(n_F - n)$, and the B species contains the other two ($|\uparrow\downarrow\rangle$, and $|0\rangle$); whereas in the second case species F consists of one more physical species ($|\uparrow\downarrow\rangle$, hence $n_{\uparrow,\downarrow} = n - n_F$), and B is just the empty state. Such difference also reflects on the degeneracy of each level of the spectrum, and ultimately manifests in a different behavior of thermodynamical quantities.
For instance, let us derive explicitly the partition function for one of the models in fig. 1, corresponding to the Hubbard model with fixed bond-charge interaction ($X = t$) (also known as AAS model [31]). Implementing the relation between n_F and $n_{\uparrow\downarrow}$, the spectrum (37) in presence of Coulomb repulsion, chemical potential, and external magnetic field becomes

$$E = E(\{n_k^{(F)}\}; N_\uparrow; N_{\uparrow\downarrow}) = \\ = \sum_k (\epsilon_k - \mu + h) n_k^F + (U - 2\mu) N_{\downarrow\uparrow} - 2h N_\uparrow \tag{45}$$

where $\epsilon_k = -2t \cos k$.
The degeneracy g corresponds to the different ways one can realize a configuration of Sutherland species, with the constraint that the total numbers $N_{\downarrow\uparrow}$ and $N_\uparrow$ appearing in (45) remain unchanged; a simple calculation yields

$$g(E(\{N_F\}; N_{\downarrow\uparrow}; N_\uparrow)) = \binom{L - N_F}{N_{\downarrow\uparrow}} \binom{N_F}{N_\uparrow} \tag{46}$$

The rearrangement of the Fock space deriving from the identification of the Sutherland Species allows a straightforward calculation of the (gran-canonical) partition function

$$\mathcal{Z} = \sum_{\{n_k^F\}} \sum_{N_{\downarrow\uparrow}=0}^{L-N_F} \sum_{N_\uparrow=0}^{N_F} g(E) e^{-\beta E(\{n_k^F\}; N_{\downarrow\uparrow}; N_\uparrow)} = \tag{47}$$

$$= (1 + e^{\beta(\mu - \frac{U}{2})})^L \prod_{k=1}^{L} \left(1 + e^{[-\beta\,(\epsilon_k - \mu^*(\mu,\beta,U,h))]}\right)$$

In the second line of (47) we have defined

$$\mu^*(\mu, \beta, U, h) = \mu + \frac{1}{\beta} \ln \frac{2 \cosh \beta h}{1 + \exp 2\beta(\mu - U/2)} \tag{48}$$

$\beta = 1/(k_B T)$ being the inverse temperature. Notice also that the product over k resulting in (47) is in form similar to the partition function of a tight binding model of spinless fermions, where μ^* plays the role of an effective chemical potential renormalized by the interaction U, the magnetic field h and the temperature itself.

By means of the partition function (47), one can calculate the thermodynamic observables from the gran potential (per site) $\omega = -\lim_{L\to\infty} k_B T \ln \mathcal{Z}$. This is done in [33]. In the following, we review the results concerning the specific heat.

In fig.3 we have plotted the specific heat (per site) C_V as a function of the temperature. Here the chemical potential μ is eliminated in favor of the filling through the relation $\rho = (n =)\partial\omega/\partial\mu$, as usual. In particular, in the top figure we have examined the case of half filling (i.e. $\rho = 1$) and zero magnetic field ($h = 0$), for different values of the on-site Coulomb repulsion U. One can observe that, across the value $U/t = 4$, the low-temperature behavior of C_V changes from linear to exponential; explicitly, for $U < 4t$ we have

$$C_V \sim \gamma T \qquad \text{with} \qquad \gamma = \frac{k_B^2 \pi}{6t\sqrt{(1 - (U/4t)^2)}}\ , \tag{49}$$

whereas for $U > 4t$

$$C_V \sim k_B \frac{(U-4t)^2}{8\sqrt{\pi}t^2}(k_BT/t)^{-3/2}\, e^{-\frac{(U-4t)}{2K_BT}} \quad . \qquad (50)$$

This is a finite-temperature effect of a metal-insulator transition, in accordance with the result obtained in [31], where a *charge* gap $\Delta_c = U - 4t$ is shown to open in the ground state for $U > 4t$. We recall that for $X = 0$ (i.e. for the ordinary 1D Hubbard model) no metal-insulator transition occurs; the bond charge term thus seems to give rise to a finite critical value U_c, increasing from 0 to $4t$ as the coupling X is varied from 0 to t.

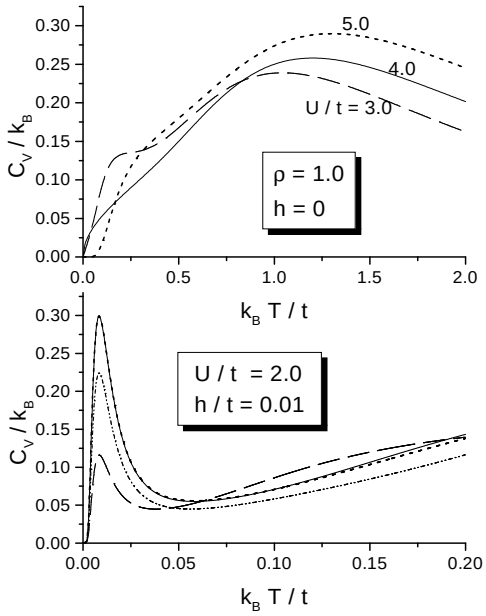

FIG. 3. The specific heat as a function of temperature. Top: $\rho = 1$, $h = 0$: the metal-insulator transition is revealed through the change in low-temperature behavior from linear to exponential across the critical value $U = 4t$.
Bottom: C_V for different filling values: $\rho = 0.25$ (dashed), $\rho = 0.50$ (dot-dashed); $\rho = 0.75$ (dotted) and $\rho = 1$ (solid); a low-temperature sharp peak emerges for non-vanishing magnetic field.

In the bottom fig.3, C_V is plotted for different filling values, fixed ratio $U/t = 2$ and magnetic field $h/t = 0.01$. A sharp low-temperature peak, located at $k_BT \sim h$, is observed to emerge as soon as the magnetic field is turned on.
One can show that

$$\lim_{T\to 0}\lim_{h\to 0} C_V/T \neq \lim_{h\to 0}\lim_{T\to 0} C_V/T \qquad (51)$$

differently from the ordinary Hubbard model, where the two limits are interchangeable [32]. At half-filling and for $|U + |2h|| < 4t$, for instance, one has $C_V \sim \gamma\, T$ with

$$\gamma = \frac{k_B^2(3\ln^2 2 + \pi^2)}{6\pi t\sqrt{(1-((U+2|h|)/4t)^2)}} \qquad (52)$$

Comparing eq.(52) to eq.(49), one can realize that (51) holds. This can be interpreted as a signal of non Fermi liquid behavior. Similarly, the exponential behavior, occurring when the gap is open, is different; namely, for $|U + |2h|| > 4t$

$$C_V \sim k_B \frac{(U+2|h|-4t)^2}{4\sqrt{\pi}t^2}(k_BT/t)^{-3/2}\, e^{-\frac{(U+2|h|-4t)}{2K_BT}} \quad . \qquad (53)$$

to be compared to eq.(50).

In fig.4 the specific heat of the Hubbard model with bond charge is plotted for $X = 1$ is aside the case $X = 0$ (i.e. the Hubbard model) for strong coupling, namely $U = 8t$.

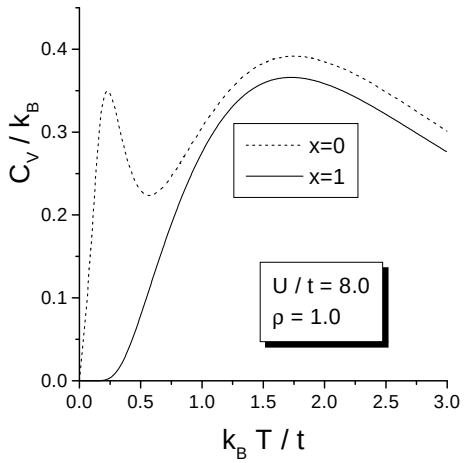

FIG. 4. The specific heat as a function of temperature for model the bond-charge model in the strong coupling regime ($U = 8t$), at half filling and zero magnetic field. The dotted line is the case $X = 0$ - i.e. the ordinary Hubbard model- obtained from [16], and the solid line the case $X = t$, obtained from our exact calculations. Continuity arguments suggest that the specific heat for arbitrary $0 \leq X \leq t$ lies between these two curves. The low-temperature peak originating from spin excitations is depleted by the bond-charge interaction.

Notice that the ordinary Hubbard model has a low-temperature peak, whose origin is due to spin degrees of freedom; the latter being not gapped, the low-temperature behavior of C_V is linear in spite of the fact that a charge gap is present at any $U > 0$ [34]. In contrast, for $X = t$ the spectrum does not carry any spin quantum number, due to the rich symmetry of the model; spins act therefore as a sort of dummy variables. Although the value $X = t$ is a particular one, it is reasonable to expect that, for continuity argument, the plot of C_V for intermediate values $0 \leq X \leq 1$ lies between the two curves. As a consequence, we can infer that the effect of spin excitations is weakened by the presence of the bond-charge interaction, at least in the strong coupling regime.

VII. APPLICATIONS TO CONSTRAINED FERMIONS MODELS

In this section we would like to discuss a simpler application of the above scheme, which is the case of two flavors electrons (up and down spin, for instance) with the constraint that no two electrons can occupy the same site (constrained fermions). The local vector space in this case has dimension $d_V = 3$, the physical species at each site being just $|\uparrow\rangle$, $|\downarrow\rangle$, and $|0\rangle$.
The more general constrained fermions Hamiltonian with nearest neighbor interaction one may think of is an extended $t-J$ Hamiltonian [10], define as

$$H_{EtJ} = -t\sum_{j,\sigma}(\tilde{c}^\dagger_{j,\sigma}\tilde{c}_{j+1,\sigma} + h.c.) + J\sum_j \vec{\mathcal{S}}_j\cdot\vec{\mathcal{S}}_{j+1} + V\sum_j \tilde{n}_j\tilde{n}_{j+1} \quad , \tag{54}$$

where $\tilde{c}_{j\sigma} \doteq (1-\hat{n}_{j,\bar{\sigma}})c_{j,\sigma}$, $\tilde{n}_{j\sigma} \doteq (1-\hat{n}_{j,\bar{\sigma}})\hat{n}_{j\sigma}$, $\bar{\sigma} = -\sigma$, and terms not conserving the total number of electrons and the total spin operator have been ignored. Interestingly, H_{EtJ} reduces to the infinite U Hubbard model for $J = V = 0$, and to the standard $t-J$ model for $V = -\frac{1}{4}$, both of which have been solved in one dimension.
Again, in order to answer the question whether there are H_{EtJ} Hamiltonians of generalized permutator type, we have to represent H_{EtJ} as a matrix, and this can be done by using the Hubbard projectors introduced in section 2 (the constraint of no double occupancy identifies in fact the 3×3 upper left submatrix of (10)). Interestingly, it turns out that the representation of the 2 sites Hamiltonian identified by (54) in this case has non-vanishing off-diagonal entries precisely where those of generalized permutators are. However, by solving the linear equations in the interaction parameters steaming from identifying such non-vanishing entries, it turns out that there are just 8 different integrable $\mathcal{H}_{EtJ}$, to be compared with the 56 different generalized permutator obtained for $d_V = 3$; the reduction of solutions being due to the required conservation of spin and charge operators.

The integrable cases can be classified according to the total number of corresponding SS into the following two classes:

$$\begin{aligned} H^{(2)}_{EtJ}(s_1,s_2) &= -t\sum_{j,\sigma}(\tilde{c}^\dagger_{j,\sigma}\tilde{c}_{j+1,\sigma} + h.c.) + (s_1+s_2)t\sum_j \tilde{n}_j\tilde{n}_{j+1} \\ H^{(3)}_{EtJ}(s_1,s_2) &= -t\sum_{j,\sigma}(\tilde{c}^\dagger_{j,\sigma}\tilde{c}_{j+1,\sigma} + h.c.) + 2s_1t\sum_j(\vec{\mathcal{S}}_j\cdot\vec{\mathcal{S}}_{j+1} - \frac{1}{4}\tilde{n}_j\tilde{n}_{j+1}) + (s_2+s_1)t\sum_j \tilde{n}_j\tilde{n}_{j+1} \quad , \end{aligned} \tag{55}$$

plus conserved quantities. Here the first group gives generalizations of the infinite U Hubbard model, the latter being obtained for $s_1 = -s_2$; whereas the second group generalizes the $t-J$ Hamiltonian, which is in fact given by the choice $s_1 = 1$, $s_2 = -1$.
Also, models in the second group all have algebraic structures of type $F^{3-l}B^l$ (these are four, in one to one correspondence with the four possible choices of signs s_1 and s_2); whereas models in the first group are of type $F^{2-l}B^l$. In particular, infinite U Hubbard model is of type FB (as expected from the known spinless fermion-like spectrum), and $t-J$ model turns out to be of type F^3.
Interestingly, while integrability of models of the second group has already been discussed in [10], apparently 2 ($V = \pm 2t$) out of the four models in the first group have not been studied elsewhere from this point of view.
Among the models of first and second type the choices of $s_1 = s_2$ are physically interesting, describing a model of interacting electrons in the limit of large on-site Coulomb repulsion and finite ($= \pm 2t$) neighboring sites Coulomb interaction. In the first group, for instance, the repulsive case ($s_1 = s_2 = 1$) corresponds to a F^2 model (the ground state and excited states of which being nicely discussed in [23]), whereas the attractive case is a B^2 model. Both should be compared with the plane infinite U Hubbard case (no Coulomb repulsion between neighboring sites), in order to understand whether neighboring sites Coulomb interaction can induce a quantum phase transition.

VIII. CONCLUSIONS

In this paper we reviewed a recently developed method to determine integrable electron models, which amounts in finding solutions of the YBE of polynomial form. The method was applied to the simpler case of first degree polynomial, and was solved in full generality in this case (for any dimension of the on-site vector space); solutions are all and only generalized permutators. These were classified in terms of Sutherland species, which allow for a complete derivation of the spectrum in the case of models of FB type, as well as for the calculation of the ground state energy in many other cases. We explicitly applied the scheme to the classification and solution of integrable electron models, both in the constrained and in the unconstrained case ($d_V = 3, 4$ respectively).
To conclude, it must be stressed that in fact the scheme developed just requires to have an Hamiltonian which –when represented in matrix form on two neighboring sites– has the same structure of a generalized permutator. Hence we expect the method to be capable of generating integrable models also in physical context different

from correlated electrons. For instance, spin S Hamiltonians have a local vector space of dimension $d_V = 2S+1$, implying that models discussed in terms of constrained fermions in the previous section could also have an interpretation as spin 1 Hamiltonian. Work is in progress along these lines.

---

[1] S. Kagoshima, H. Nagasawa, T. Sambongi, *One-dimensional Conductors*, Springer Berlin (1982)

[2] D.K. Campbell, J.T. Gammel and E.Y. Loh Jr, Phys. Rev B **42**, 475 (1990)

[3] C. Bourbonnais, D. Jerome, Phys. World **11**, 41 (1998)

[4] R. Egger and A. O. Gogolin Phys. Rev. Lett. **79**, 5082 (1997); C. Dekker, Physics Today **52(5)**, 22 (1999).

[5] S.Tarucha and T. Honda and T. Saku, Solid State Comm., **94**, 413 (1995); A. Yacoby *et al.*, Solid State Comm., **101**, 77 (19956); A. Yacoby *et al.*, Phys. Rev. Lett., **77**, 4612 (1996).

[6] J. Voit, Rep. Prog. Phys. **58**, 977 (1995); J. von Delft, H. Schöller, Annalen Phys. **7**,225 (1998); A. O. Gogolin, A. A. Nersesyan, and A. M. Tsvelik, *Bosonization and Strongly Correlated Systems* (Cambridge University Press, Cambridge, 1998).

[7] S. R. White and R. M. Noack Phys. Rev. Lett. **68**, 3487(1992); K. Hallberg, "Density Matrix Renormalization: A Review of the Method and its Applications", *Theoretical Methods for Strongly Correlated Electrons*, CRM Series in Mathematical Physics, eds. D. Sénéchal, A.-M. Tremblay and C. Bourbonnais, Springer, New York, 2003

[8] M. Gaudin, *La fonction d'onde de Bethe* (Masson, 1983); Z. N. C. Ha, *Quantum many-body systems in one-dimension* (World Scientific, 1996); N. Andrei, *Integrable Models in condensed matter physics*, cond-mat/9408101

[9] J. Hubbard, *Proc Roy. Soc. London*, Sec. *A* **276**, 238 (1963); *The Hubbard Model, a reprint volume*, edited by A. Montorsi, World Scientific (1992); *The Hubbard Model, recent result*, edited by M. Rasetti, Series on Advances in Statistical Mechanics, World Scientific (1991); M.Takahashi, *Thermodynamics od one-simensional solvable models*, Cambridge University Press 1999; T. Deguchi *et al.* Phys. Rep. **331**, 197 (2000)

[10] P.A. Bares, G. Blatter, Phys. Rev. Lett, **64** (1990), 2567; N. Kawakami, S. K. Yang, Phys. Rev. Lett. **65** (1990), 2309; J. Phys. Cond. Mat. **3** (1991), 5983; M. Ogata *et al.*, Phys. Rev. Lett, **66**, 2388 (1991); P. Schlotmann, Phys. Rev. B **36**, 5177 (1987)

[11] F.C. Zhang, T.M. Rice, Phys. Rev. B **37** (1988), 3759

[12] V.J. Emery, *Correlated Electron Systems*, Jerusalem Winter School for Theoretical Physics, vol. 9, World Scientific (1993)

[13] V. E. Korepin and F. Essler, *Exactly solvable models of strongly correlated electrons*, Advanced Series in Mathematical Physics 18 (World Scientific, Singapore, 1994)

[14] V.E. Korepin, N.M. Bogolubov, and A.G. Izergin, *Quantum Inverse Scattering Method and Correlation Functions* (Cambridge University Press, 1993); P.P. Kulish, E.K.Sklyanin, J.Sov.Math. **19** (1982) 1596; L.D. Faddeev, in *Integrable Systems*, Nankai Lectures on Mathematical Physics (World Scientific, Singapore, 1990); F.C. Pu, B.H. Zhao, in *Integrable Systems*, Nankai Lectures on Mathematical Physics (World Scientific, Singapore, 1990)

[15] F. Dolcini, A. Montorsi, Int.J.Mod.Phys. B **13** (1999) 2953

[16] F.Dolcini, A. Montorsi, Int. J. Mod.Phys. **B 14**, 1719 (2000)

[17] In the case of s-orbital electrons we thus have $h_j^{(1)} = c_{j,\uparrow}^\dagger$; $h_j^{(2)} = c_{j,\downarrow}^\dagger$; $h_j^{(3)} = 1$; $h_j^{(4)} = c_{j,\downarrow}^\dagger c_{j,\uparrow}^\dagger$

[18] Due to the order defined by eq.(5) we have $p(1) = p(2) = 1$ and $p(3) = p(4) = 0$.

[19] F. Göhmann, and S. Murakami, J. Phys. A **31**, 7729 (1998)

[20] F.Dolcini, A. Montorsi, Nucl.Phys. **B 592**, 563 (2001)

[21] P.P. Kulish, E.K. Sklyanin, J.Sov.Math **19**, 1596 (1982)

[22] J. Hietarinta, Phys. Lett. A **165**, 245 (1992)

[23] B. Sutherland, Phys. Rev. B **12**, 3795 (1975)

[24] P.P. Kulish, N. Yu. Reshetikhin, Sov. Phys. JETP **53** (1) (1981) 108

[25] A. Förster, M. Karowski, Nucl. Phys. B **396** (1993) 611

[26] F.H. Essler, and V.E. Korepin, Phys. Rev. B**46** (1992) 9147

[27] F.H. Essler, V. Korepin, and K. Schoutens, Phys. Rev. Lett. **68**, 2960 (1992); Phys. Rev. Lett. **70**, 73 (1993)

[28] F. Dolcini, and A. Montorsi, Phys. Rev. B**63** 121103 (2001)

[29] J. de Boer, V. Korepin, A. Schadschneider, Phys. Rev. Lett. **74**, 789 (1995); C. Castellani, C. Di Castro, M. Grilli, Phys. Rev. Lett. **72**, 3626 (1994)

[30] A.J. Bracken et al, J. Phys. A **34**, 4459 (2001)

[31] L. Arrachea, and A.A. Aligia, Phys. Rev. Lett. **73**, 2240 (1994); A. Schadschneider, Phys. Rev. B **51**, 10386 (1995)

[32] M. Takahashi, Prog. Theor. Phys. **52**, 103 (1974)

[33] F. Dolcini, and A. Montorsi, Phys. Rev. B**65**, 155105 (2002); Phys. Rev. B**66**, 075112 (2002)

[34] E.H. Lieb, and F.Y. Wu, Phys. Rev. Lett. **20**, 1443 (1968)